

Microstructural Evolution and Mechanical Properties of Ultrafine/nano Structured AISI 321 Stainless Steel Produced by Thermo-mechanical Processing

M. Golzar Shahri ^{1*}, M. Salehi ², S. R. Hosseini ³

^{1,2} Department of Materials Engineering, Isfahan University of Technology, Isfahan 84156-83111, Iran.

³ Department of Materials Engineering, Maleke-ashtar University of Technology, Isfahan 83145-115, Iran.

Abstract

The mechanical properties and microstructural developments of 321 stainless steel during thermo-mechanical process were investigated. The repetitive cold rolling and subsequent annealing were conducted to achieve nanocrystalline structure in an AISI 321 stainless steel. Heavily cold rolling at -20°C was conducted to form martensite in metastable austenitic steel. The process was followed by annealing treatment at $700\text{--}850^{\circ}\text{C}$ for $0.5\text{--}30$ min. The effects of process parameters such as “reduction percentage”, “annealing temperature”, and “annealing time” on the microstructural development were also investigated. Microstructural evolutions were conducted using ferroscope, X-ray diffraction and scanning electron microscope (SEM). The mechanical properties were determined by hardness (Vickers method) and tensile test. The results indicated that more thickness reduction made more martensite formation, leading to the rise of hardness. In addition, mechanical evaluations after heat treatments revealed that decreasing austenite grain size to $0.7\ \mu\text{m}$ resulted in hardness and strength increment by adapting Hall-Petch equation.

Keywords: Austenitic stainless steel, Deformation induced martensite, Nano/ultrafine grain structure, Thermo-mechanical treatment, Hall-Petch relationship.

1. Introduction

Austenitic stainless steels (ASSs) have many advantages from a metallurgical point of view. Alloy 321 is stabilized stainless steel offered as some excellent resistance to intergranular corrosion. Alloy 321 has also advantages for high temperature services ¹⁾. In recent years, there has been an interest in developing nano/ultrafine grain stainless steels to obtain high strength/good ductility alloys. For this purpose, several techniques have been used, including advanced thermo-mechanical treatment (ATP) and severe plastic deformation (SPD) techniques such as high pressure torsion (HPT), equal channel angular pressing (ECAP) and accumulative roll bonding (ARB). Tomimura et al. ²⁻⁴⁾ have suggested a novel thermo-mechanical process consisting of heavy cold rolling and subsequent annealing. The alloys used in their investigation were an Fe-18Cr-8.65Ni alloy and two metastable austenitic stainless steels, 15.6Cr-9.8Ni (the 16Cr-10Ni) and 17.6Cr-8.8Ni (the 18Cr-9Ni). Ma et

al. ⁵⁾ have provided nanocrystalline grains (about 200 nm in diameter) in a metastable austenitic steel by a repetitive thermo-mechanical process. This austenitic steel exhibits not only high strength (above 1 GPa), but also good elongation (above 30%). Rajasekhara et al. ⁶⁾ created ultra-fine austenite grains as small as $0.54\ \mu\text{m}$ in AISI 301LN stainless steel. Tensile tests revealed a very high yield strength of about 700 MPa, which was twice the typical yield strength of conventional fully annealed steels. They claimed that the relationship between yield strength and grain size in these submicron-grained stainless steels indicated a classical Hall-Petch behavior.

In all above investigations, a metastable ASS has been processed using ATP to nanostructure formation. In other words, stable ASSs like AISI 321 have not been processed to produce nanocrystalline grains and investigate their behavior. So, this work focused on the effects of the thermo-mechanical parameters on the mechanical properties and microstructural developments of AISI 321. Moreover, the relationship between austenite grain size and mechanical properties was evaluated.

2. Materials and Experimental Procedures

The chemical composition of AISI 321 metastable ASS used in this investigation is shown in Table 1.

Corresponding author

Tel: +98 913 351 0175

Email: m.golzar@ma.iut.ac.ir

Address: Department of Materials Engineering, Isfahan University of Technology, Isfahan 84156-83111, Iran.

1. PhD Student

2. Professor

3. Assistant Professor

Table 1. Chemical composition (wt. %) of AISI 321 stainless steel used in the present work.

C	Mn	Si	Cr	Ni	Ti	Mo	S	P	Fe
0.07	1.22	0.75	17.9	9.3	0.36	0.15	0.003	0.04	Rem

Hot rolled steel strips with 10 mm initial thickness were rolled using 90% thickness reduction at -20°C . The thickness reduction in each pass was 0.2 mm. The specimens were cooled in methanol, salt and ice mixture (-20°C) before each pass. The annealing treatments were followed by cold rolling. Annealing treatment was performed using an electrical furnace at 700, 750, 800 and 850°C , for 1, 2, 3, 4, 5, 7, 10, 12, 15, 20 and 30 min. Specimens were subsequently water quenched after the heat treatments.

The specimen microstructures were revealed by an optical microscope (OM, Olympus GX71) and a scanning electron microscope (SEM, COXEM CX100).

The amount of deformation induced martensite (DIM) was measured using X-ray diffractometer (STOE STADI P, Cu $K\alpha$ target, $\lambda= 1.54184 \text{ \AA}$, the focus line of $0.4 \times 12 \text{ mm}$ and the exposure time of 10 min) and Feritscope (Fischer FMP30). Hardness measuring was conducted by Vickers method (HV) using a Wilson Wolpert tester 930/250 universal hardness machine with the indenting load of 10 kgf. Hardness of each sample was reported as a mean value at five measurements. Tensile properties were evaluated by Santam testing machine (STM 50) with the 1 mm/min cross head speed.

3. Results and Discussion

The effect of thickness reduction on DIM percentage at -20°C is shown in Fig. 1. As can be seen, more deformation provided more DIM deformation. Besides, this figure indicates that austenite to martensite phase transformation was completed at 60% thickness reduction. Therefore, saturated strain (ϵ_s) was calculated to be about 0.9. Saturated strain can be calculated by following equation:

$$\epsilon_s = \ln \frac{1}{1-r} \quad (\text{Eq. 1})$$

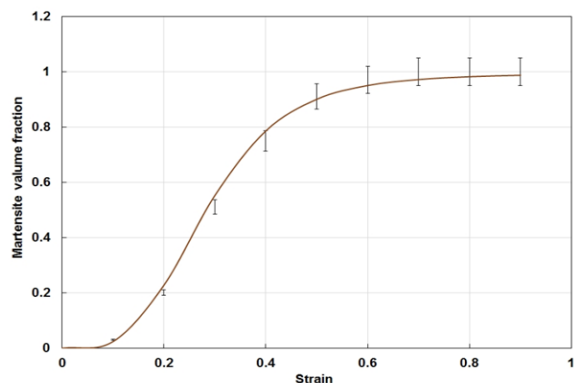


Fig. 1. The effect of thickness reduction (Strain) on the martensite formation during cold rolling.

In this equation, (ϵ_s) is the saturated strain and r is the thickness reduction. As shown in Fig. 1, transformation curve was divided into three stages. The first stage was up to 10% thickness reduction. In this stage, cold work energy was mostly consumed to deformation and the transformation rate was very low. The second stage began from 10% thickness reduction to ϵ_s (60% thickness reduction). In this stage, the transformation rate was increased by strain increment. At the end of this stage, austenite to martensite phase transformation was completed. In the last stage (after ϵ_s), the martensite percentage was constant, because austenite was completely replaced by DIM and more reduction led to crushing DIM.

The α' -martensite measurement data of AISI 321 steel was analyzed using Olson-Cohen theory ⁷. The theory recommends an equation to explain the relationship between the volume fraction of α' -martensite (f_a) and strain (ϵ):

$$f_a = 1 - \text{Exp} \{-\beta [1 - \text{Exp}(-\alpha\epsilon)]^n\} \quad (\text{Eq. 2})$$

Where α and β are temperature dependent parameters and n is a constant. The parameter α describes the path of shear band formation and it is dependent on the stacking fault energy (SFE). The temperature dependence of the parameter is due to the fact that the SFE depends on the temperature. The parameter β is proportional to the possibility of the nucleation of an embryo of α' -martensite at a shear band intersection.

As the chemical driving force of α' -martensite formation is dependent on the temperature, β is temperature dependent as well. The fitting results supported quite well the Olsen-Cohen model. The data were fitted by the Eq. (2) in Fig. 1 with $\alpha= 3.6$, $\beta= 5.2$, and $n = 4.5$, while $r^2 = 0.998$.

The XRD patterns of the specimens after different cold rolled reductions, as compared to as-received materials, are represented in Fig. 2. Induction of austenite to α' -martensite transformation as a result of cold rolling was confirmed by the XRD patterns shown Fig. 2.

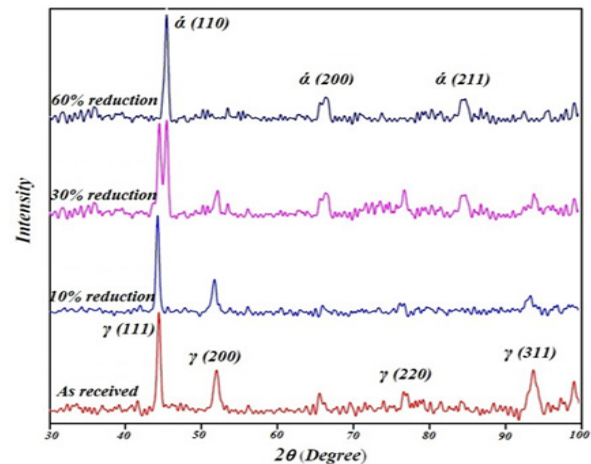


Fig. 2. The XRD patterns of specimens after different cold reductions.

For the as-received sample, austenite main peaks were related to the planes (111), (200), (220) and (311), which were created in the diffraction angles of $2\theta = 44.5, 64.5, 83$ and 95.5 degree, respectively.

It was clear that the as-received steel had austenitic structure. Up to 10% thickness reduction, cold work only led to plastic deformation without any significant phase transformation. Regarding this issue, more induced martensite was formed as a consequence of extending thickness reduction. The main reason for induced martensite formation was the creation of martensite peaks related to the planes (111), (200) and (211) after 30% thickness reduction. Moreover, the XRD pattern of steel after 30% thickness reduction illustrated that austenite and martensite main peak intensities were approximately equal, so the volume percentage of both phases was fairly equal. Therefore, M_d^{30} (the temperature at which 50% martensite could be formed at 30% true strain) was estimated to be about -20°C (rolling temperature). After 60% thickness reduction, all main peaks of α -martensite, i.e., (110), (200) and (211), were represented, so martensite became the main phase. Further cold work could only lead to crushing the martensite lathes.

Fig. 3 shows the hardness values versus thickness reduction during the cold rolling. As can be seen, hardness was increased from 200 HV to about 490 HV when the thickness reduction was increased from zero to 90%. The rate of hardness rise was high at the beginning of thickness reduction. This could be attributed to the austenite to martensite transformation at lower thickness reduction up to the saturated strain. However, more reduction only led to crushing DIM and increasing the dislocation density. Martensite crushing had less effect on hardness increment than martensite formation. So, at the end of thickness reduction (from ϵ_s to 90% thickness reduction), hardness curve had a lower slope.

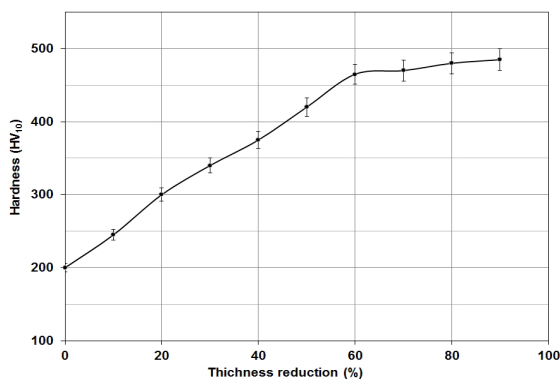


Fig. 3. The effect of Annealing time and temperature on the hardness after annealing.

To investigate the mechanical properties and their relationship with austenite grain size, several grain sizes were produced using different annealing procedures. The results illustrated that when annealing time

was increased, the grain size became greater; especially, within 8 min, the grains grew suddenly. Grain sizes after 8 and 15 min annealing were calculated to be about 0.7 and 3.5 μm , respectively (Fig. 4).

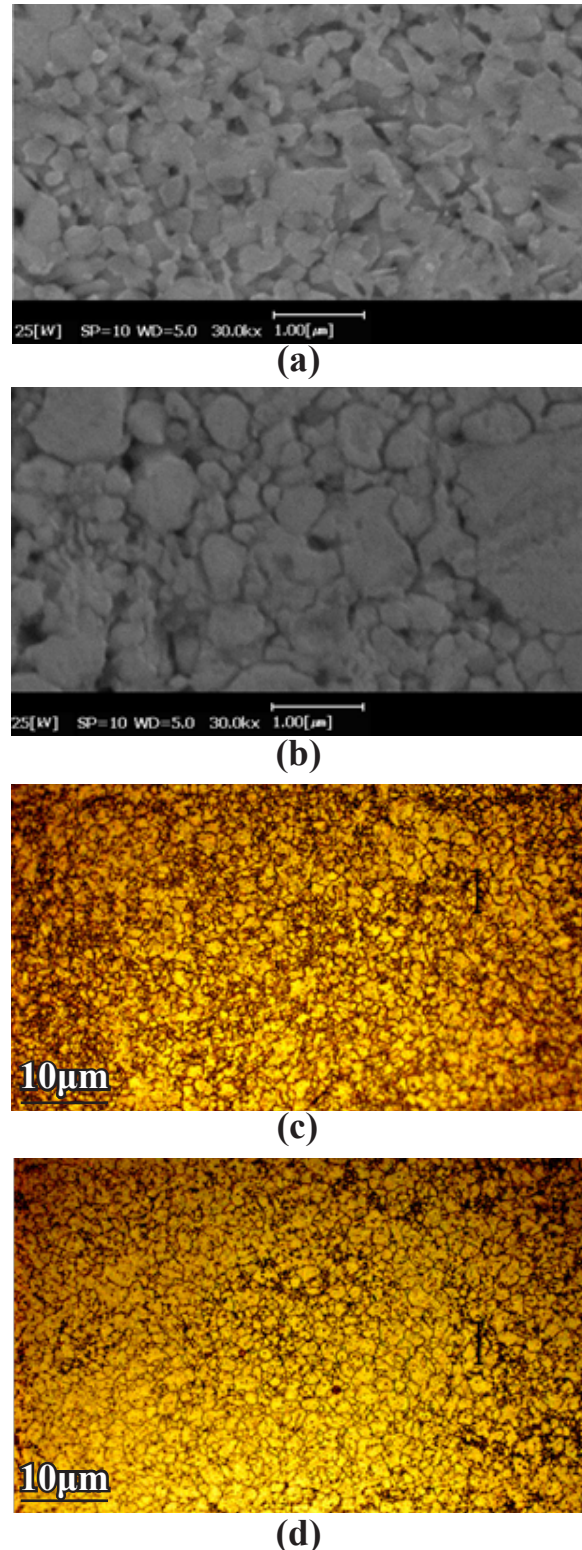


Fig. 4. (a) and (b): SEM micrographs of the specimens annealed at 800°C for 3 and 8 min, respectively; (c) and (d): Optical micrographs of the specimens annealed at 800°C for 15 and 25 min, respectively.

Fig. 5 presents the tensile properties of 321 ASS as a function of grain size. Also, Table 2 shows the computed mechanical properties along with microstructural features. As can be seen, decreasing the grain size led to increasing hardness and strength, unlike elongation percentage.

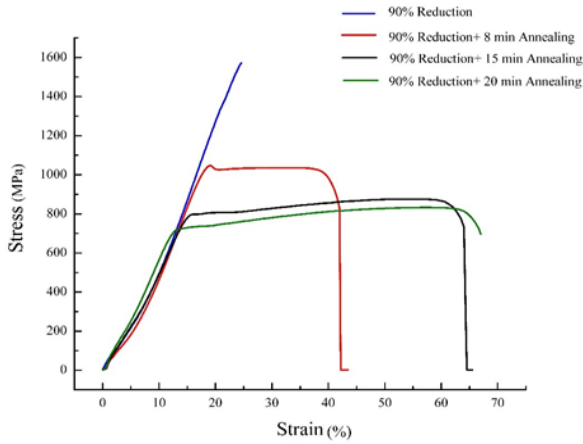


Fig. 5. Engineering stress-strain curves of the specimens under different grain sizes.

Table 2. The effects of different processing parameters on the mechanical properties of 321 nano-ultrafine steel.

Process procedure	Average grain size (μm)	Hardness (HV10)	Yield strength (MPa)		UTS (MPa) Exp.	Elongation (%)	structure
			Th.	Exp.			
As received steel	45	170	555	570	710	52	γ
90% CR at -20°C	-	480	1570	1600	1600	1.6	α
90% CR at -20°C, annealed at 800°C/3min	0.15	380	1280	1250	1320	14	γ/α
90% CR at -20°C, annealed at 800°C/8min	0.7	295	965	1000	1050	20	γ
90% CR at -20°C, annealed at 800°C/15min	3.5	235	770	820	870	34	γ
90% CR at -20°C, annealed at 800°C/25min	4	215	700	720	830	46	γ

Theoretical values for yield strength in Table 2 were achieved by the following equation⁸⁾:

$$\sigma_y = 9.8(HV)/3 \quad (\text{Eq. 3})$$

In this equation, σ_y is the yield strength and HV is the Vickers hardness. As observed in this table, experimental results conformed well with the theoretical values. The yield strength of about 1300 MPa could be

achieved by annealing at 800°C for 3 min, which was nearly three times higher than that of the as received steel. As mentioned before, many investigations have attempted to evaluate the mechanical properties of nanostructured materials. The results obtained were rather contradictory. For example, in some works⁹⁻¹²⁾, a negative deviation from the Hall-Petch relationship (Eq. 4) was observed in the case of small grains while in others¹³⁻¹⁵⁾, an opposite tendency was revealed.

$$HV = HV_0 + KD^{-0.5} \quad (\text{Eq. 4})$$

In this equation, D is the grain size, HV is the Vickers hardness, HV_0 is a constant which depends on the hardness of a single crystal and K is a constant for a material with a single phase. The results indicated that decreasing grain size from 45 μm to 0.7 μm caused the increase hardness with good conformity to the Hall-Petch relationship. Fig. 6 presents the Hall-Petch equation curve for the stainless steel studied in the present work. In other words, this curve shows the hardness as a function of $D^{-0.5}$. However, under 0.7 μm grain size, material behavior (especially hardness) showed an obvious deviation from Hall-Petch relationship. So, the Hall-Petch curve was divided into two stages. In the first stage (from 45 μm to 0.7 μm), hardness had a very good conformity with Hall-Petch relationship. Calculated parameters, i.e., curve slope (K), was determined to be about 4 and HV_0 was estimated to be about 170. However, in the second stage (grains finer than 0.7 μm), the curve slope (K) was calculated about 0.3. So, hardness increment rate in the second stage was much less than that of the first stage.

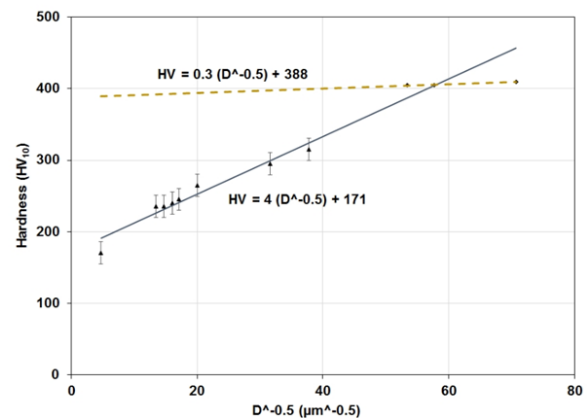


Fig. 6. Hardness of 321 ASS as a function of grain size (Hall-Petch equation curve).

4. Conclusion

During the cold work, the formation of α-martensite phase began after 10% deformation and before that, cold work consumed grain elongation. After 30% deformation, the volume percentage of both austenite and martensite phases was nearly equal, so M_d^{30} was estimated to be about -20°C (rolling temperature). Finally,

the metastable austenite was completely transformed to the α -martensite after 60% deformation. The strain-induced martensite transformation curve, based on experimental data, had a good agreement with the Olsen–Cohen theory. The parameters of the model for AISI 321 stainless steel were $\alpha = 3.6$, $\beta = 5.2$, and $n = 4.5$ for -20°C . Decreasing the grain size in 321 ASS led to improving the mechanical properties with good conformity to Hall-Petch relationship, down to $0.7\ \mu\text{m}$ grain diameter. For this region, K and HV_0 were calculated to be about 4 and 170 respectively. However, under $0.7\ \mu\text{m}$ grain diameter, material behavior and Hall-Petch constant were changed. In other words, under $0.7\ \mu\text{m}$ grain diameter, K was calculated to be about 0.3.

References

- [1] M. Mc Guire, *Stainless steel for design engineers*, first printing, ASM International, Materials Park Ohio, (2008).
- [2] K. Tomimura, S. Takaki, S. Tanimoto and Y. Tokunaga: *ISIJ. Int.*, 31(1991), 721.
- [3] S. Takaki, K. Tomimura and S. Ueda: *ISIJ. Int.*, 34(1994), 522.
- [4] K. Tomimura, S. Takaki and Y. Tokunaga: *ISIJ. Int.*, 31(1991), 1431.
- [5] Y. Ma, J. Jin and Y. Lee: *Scr. Mat.* 52(2005), 1311.
- [6] S. Rajasekharaa, P. J. Ferreira, L. P. Karjalainen, and A. Kyröläinen: *Metal. Mater. Trans. A.*, 38A(2007), 1202.
- [7] G.B. Olsen, and M. Cohen: *Metall. Trans.*, 6A(1975), 791.
- [8] D. Tabor, *The hardness of metals*, Oxford, UK, Oxford University Press, (1952).
- [9] A. H. Chokshi, A. Rosen, J. Karch and H. Gleiter: *Scr. Metal.* 23(1989), 1679.
- [10] K. A. Padmanabhan, S. Sripathi, H. Hahn and H. Gleiter: *Mater. Lett.* 133(2014), 151.
- [11] T. Christman and M. Jain: *Scr. Metal. Mater.*, 25(1991), 767.
- [12] K. S. Kumar, H. Van Swygenhoven and S. Suresh: *Acta. Mater.*, 51(2003), 5743.
- [13] G. W. Nieman, J. R. Weertman and R. W. Siegal: *Scr. Metal.* 23(1989), 2013.
- [14] A. M. El-Sherik, U. Erb, G. Palumbo and K.T. Aust: *Scr. Metal. Mater.*, 27(1992), 1185.
- [15] M. Y. Seok, I. Choi, J. Moon, S. Kim, U. Ramamurtyd and J. Jang: *Scri. Mater.* 87(2014), 49.